Proceedings of IMECE2004:
2004 ASME International Mechanical Engineering Congress
November 13-19, 2004, Anaheim, CA USA

IMECE2004-60231

SIMULTANEOUS OPTIMIZATION OF REMOVAL RATE AND PART ACCURACY IN HIGH-SPEED MILLING

Mohammad H. Kurdi
Dept. of Mechanical and Aerospace Engineering,
University of Florida, Gainesville, FL

Raphael T. Haftka
Dept. of Mechanical and Aerospace Engineering,
University of Florida, Gainesville, FL

Tony L. Schmitz
Dept. of Mechanical and Aerospace Engineering,
University of Florida, Gainesville, FL

Brian P. Mann
Dept. of Mechanical and Aerospace Engineering,
University of Florida, Gainesville, FL

ABSTRACT

High-speed milling provides an efficient method for accurate discrete part fabrication. However, successful implementation requires the selection of appropriate operating parameters. Balancing the multiple process requirements, including high material removal rate, maximum part accuracy, sufficient tool life, chatter avoidance, and adequate surface finish, to arrive at an optimum solution is difficult without the aid of an optimization framework. In this paper, an initial effort is made to apply analytical tools to the selection of optimum cutting parameters (spindle speed and depth of cut are considered at this stage). Two objectives are addressed, maximum removal rates and minimum surface location error. The Time Finite Element Analysis method is used in the optimization algorithm. Sensitivity of the surface location error to small changes in spindle speed near tooth passing frequencies that are integer fractions of the system's natural frequency corresponding to the most flexible mode is calculated. Results of the optimization algorithm are verified by experiment.

1 INTRODUCTION

Intense competition in manufacturing places a continuous demand on developing cost-effective manufacturing processes with acceptable dimensional accuracy. High-speed milling offers these benefits provided appropriate operating parameters are selected. Some typical applications include, but are not limited to, end milling (pocketing) of airframe panels and ball end milling of stamping dies in automotive manufacturing.

However, the selection of these preferred operating conditions is not trivial. Existing barriers to the full realization of the potential productivity gains in manufacturing environments include: 1) the requirement for multiple tool point dynamic measurements; 2) sensitivity of part quality to small changes in process variables; and 3) the difficulty in concurrently considering stability, accuracy, and surface finish in an analytical framework. Therefore, balancing the multiple requirements, including high material removal rate, f_{MRR}, minimum surface location error $\left|f_{SLE}\right|$, sufficient tool life, chatter avoidance, and adequate surface finish, to arrive at an optimum solution is difficult without the aid of optimization techniques.

Previous research in machining process optimization has focused on mathematical modeling approaches to determine optimal cutting parameters with regard to various objective functions. Three main objectives have been recognized: 1) maximum production rate or minimum cycle time; 2) minimum cost [1-4]; and 3) maximum profit [5, 6], or a combined criterion based on a weighted sum of these [7].

Several techniques have been used to handle the machining optimization problem [8], including classical linear and nonlinear programming [9, 10], the probabilistic approach [2, 11-14], polynomial geometric programming [15-19], geometric programming based on quadratic polylog-nomials (QPL) [20], goal programming with linear [21-23] and nonlinear [24] goals and Fuzzy optimization [25, 26]. A recent study used particle swarm optimization for optimization of NC milling [27].

Jha [28] studied multiple objective function optimization based on cost and rate of production where example constraints were machine power, cutting speed limitations, depth of cut, and table feed. However, the two objectives were combined using weights. Koulams [29] studied single-pass machining considering the influence of tool chatter failure where a tool failure probability function effect was added as a penalty cost function to the objective function. Armarego *et al.* [30] considered cost optimization for single-pass rough peripheral milling while observing various practical machine tool

constraints, such as maximum available power, torque, feed force, feed rate, and cutting speed limits. Armarego *et al*. [31] also studied multi-pass peripheral and end milling to maximize production rate under a range of constraints relevant to rough milling.

Akturk *et al.* [32] optimized the production cost for a multi-pass turning operation, considering machining parameters and tool allocation simultaneously. Sonmez *et al*. [33] developed a strategy to determine the optimum cutting parameters for multi-pass milling operations based on a 'maximum production rate' criterion using geometric programming. Wang *et al.* [34] analyzed single-pass face milling based on a maximum production rate criterion within the machine tool constraints; also, surface roughness for finishing operation was considered. Lin [35] proposed an optimization technique for face milling stainless steel based on the Taguchi method where cutting speed, feed rate, and depth of cut were optimized using removed volume, surface roughness, and burr height.

A recent study by Kim *et al*. [36] focused on optimizing cutting speed to improve machining accuracy and tool life in high-speed ball end milling. Also Juan *et al*. [37] applied the concept of adaptive learning (polynomial network) to select optimum cutting speed parameters such as cutting speed, chip load, axial depth of cut, and radial depth of cut to minimize production cost for rough high-speed machining operations. In a more recent analysis, Lu *et al*. [38] presented a model for contour turning where, in contrast to previous research, process stability, force variation, and tool geometry were accommodated as constraints, in addition to machining parameters such as cutting speed, feed rate, and depth of cut.

Multi-objective optimization addresses the issue of competing objectives using concepts developed by Pareto [39], the French-Italian economist who established an optimality concept in the field of economics based on multiple objectives. A Pareto front [40] is generated that allows designers to trade off one objective against others. The efficiency of the optimization process is highly affected by the objective functions and constraints solution techniques. The Temporal Finite Element Analysis (TFEA) [41-45] approach is used here to obtain rapid process performance calculations of surface location error f_{SLE} and stability. The computational efficiency of TFEA compared to conventional time-domain simulation methods, in addition to the clear and distinct definition of stability boundaries (i.e., eigenvalues of the milling equation with an absolute value greater than one identify unstable conditions, see Section 2), makes it the most attractive candidate for use in the optimization algorithm.

In this paper, an initial effort to apply analytical tools that find optimum cutting parameters (spindle speed, Ω and axial depth of cut, *b*, for peripheral end milling operations are considered at this stage) is attempted. Two objectives are addressed, f_{MRR} and $\left|f_{SLE}\right|$, where only stability and side constraints of the design variables are considered. At this stage, no consideration is given to limitations of spindle power, torque or tool strength. The tradeoff method [46] is used to generate the Pareto front of f_{MRR} and $\left|f_{SLE}\right|$. Here, the two-objective problem is transformed into a series of single objective problems by establishing a set of different limits on the second objective. Solution of the optimization problem is performed using Matlab's Sequential Quadratic Programming algorithm (SQP) and Particle Swarm Optimization (PSO) [47].

The paper is organized as follows: Section 2 gives the milling model description and solution technique; Section 3 defines the optimization problem standard form and optimization methods used; Section 4 describes the experimental verification; and Section 5 summarizes the main conclusions of the paper.

2 MILLING MODEL

The schematic for a two-degree of freedom (2-DOF) milling process is shown in *Figure 1*. With the assumption of either a compliant tool or structure, a summation of forces gives the following equation of motion:

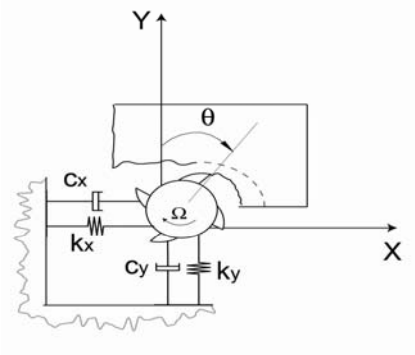

Figure 1. Schematic of 2-DOF milling tool.

$$\begin{bmatrix} m_x & 0 \\ 0 & m_y \end{bmatrix}\begin{Bmatrix} \ddot{x}(t) \\ \ddot{y}(t) \end{Bmatrix} + \begin{bmatrix} c_x & 0 \\ 0 & c_y \end{bmatrix}\begin{Bmatrix} \dot{x}(t) \\ \dot{y}(t) \end{Bmatrix} + \begin{bmatrix} k_x & 0 \\ 0 & k_y \end{bmatrix}\begin{Bmatrix} x(t) \\ y(t) \end{Bmatrix} = \begin{Bmatrix} F_x(t) \\ F_y(t) \end{Bmatrix}, \quad (1)$$

where the terms $m_{x,y}$, $c_{x,y}$, and $k_{x,y}$ are the modal mass, viscous damping, and stiffness terms and $F_{x,y}$ are the cutting forces in the *x* and *y* directions, respectively. A compact form of the milling process can be found by considering the chip thickness variation and forces on each tooth (a detailed derivation is provided in references [41-45]):

$$\mathbf{M}\ddot{\vec{X}}(t)+\mathbf{C}\dot{\vec{X}}(t)+\mathbf{K}\vec{X}(t)=\mathbf{K_c}(t)b\left(\vec{X}(t)-\vec{X}(t-\tau)\right)+\vec{f}_o(t)b\,, \quad (2)$$

where $\vec{X}(t)=\left[x(t)\quad y(t)\right]^T$ is the two-element position vector and **M**, **C**, and **K** are the 2x2 modal mass, damping, and stiffness matrices, $\mathbf{K_c}$ and $\vec{f}_0$ are defined in references [41-45], $\tau = 60/(N\Omega)$ is the tooth passing period, Ω is the spindle speed given in rev/min (rpm), and N is the number of teeth on the cutting tool.

TFEA [41-45] is used here to transform Eq. (2) into a discrete linear map. Stability of the milling process can be determined using eigenvalues of the dynamic map, while surface location error (see *Figure 2*) is found from the fixed points of the dynamic map. Details can be found in references [41-45].

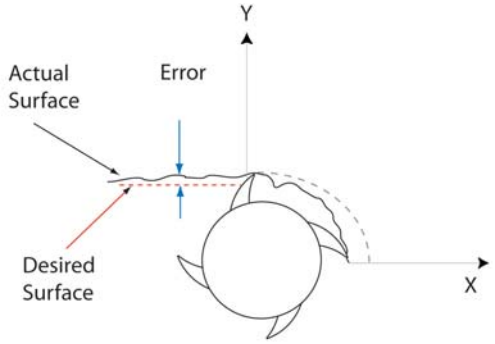

Figure 2. Up-milling schematic showing surface location error in milling as a result of cutting tool vibrations.

3 OPTIMIZATION PROBLEM STATEMENT

The problem of minimizing surface location error $\left|f_{SLE}\right|$ and maximizing material removal rate f_{MRR} is stated as follows:

$$\min_{\vec{x}\in X}\left[\left|f_{SLE}\left(x_1,x_2\right)\right|\,,\ -f_{MRR}\left(x_1,x_2\right)\right] \quad (3)$$

$$\text{Subject to: } g_\lambda\left(x_1,x_2\right):\max\left|\vec{\lambda}\left(x_1,x_2\right)\right|\le 1 \quad (4)$$

where x_1 is the axial depth of cut, x_2 is the spindle speed, g_λ is the stability constraint obtained from the dynamic map eigenvalues, f_{SLE} is found from the fixed points, and f_{MRR} is given as:

$$f_{MRR}\left(x_1,x_2\right)=Cx_1x_2 \quad (5)$$

where C depends on the feed per tooth, N, and radial depth of cut.

3.1 Tradeoff method

As shown in *Figure 3*, the Pareto front is comprised of a set of optimal points such that in moving from point A to point B in the set, any improvement in one of the objective functions from its current value would cause at least one of the other objective functions to deteriorate from its current value [47]. Based on this definition, point C is not on the Pareto front (i.e., it is a dominated point), while points A and B belong to the non-dominated set (Pareto optimal set). In essence, the front defines a limit beyond which the Pareto solutions cannot be further improved with respect to all objectives simultaneously [48].

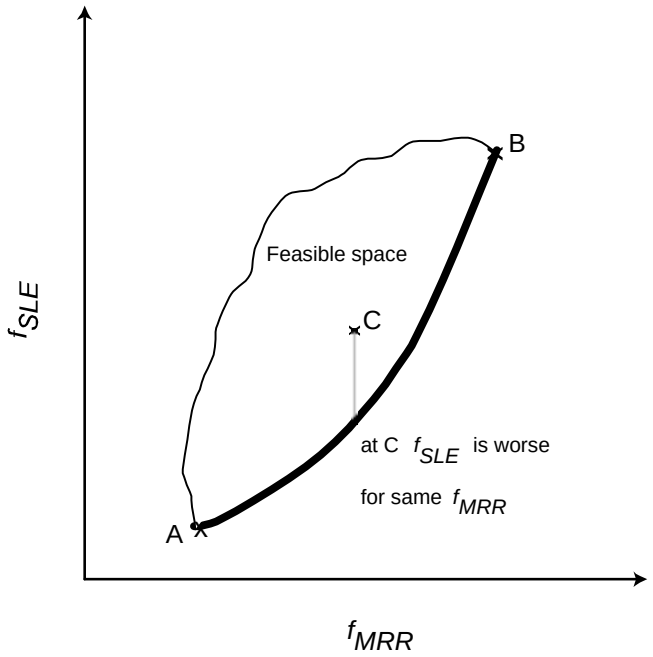

Figure 3. Typical Pareto front as per [48].

As noted, to address the multi-objective problem the tradeoff method is used, where the two-objective problem is transformed into a single objective problem of minimizing one objective with a set of different limits on the second objective. Each time the single objective problem is solved, the second objective is constrained to a specific value until a complete set of optimum points are found that are used to generate the Pareto front [40] of the two objectives. Each point on the Pareto front locates an optimum point of the two objectives in the design space. The transformed form of the problem becomes:

$$\min_{\vec{x}\in X} -f_{MRR}\left(x_1, x_2\right) \tag{6}$$

$$\text{Subject to: } \left|f_{SLE}\left(x_1, x_2\right)\right| \le \varepsilon_i \quad \text{for } i = 1, ..., k \tag{7}$$

$$g_\lambda\left(x_1, x_2\right) : \max\left|\vec{\lambda}\left(x_1, x_2\right)\right| \le 1 \tag{8}$$

for a series of selected limits (ε) on f_{SLE} .

3.2 Robust Optimization: SQP vs. PSO

Two optimization algorithms were used to solve the two-objective problem, namely Sequential Quadratic Programming (SQP) using Matlab functions and Particle Swarm Optimization (PSO). The former is a local, gradient-based search method, while the latter is a global, non-gradient-based approach. In generating the Pareto front for this problem using the SQP algorithm, the minimum $\left|f_{SLE}\right|$ points were found to favor spindle speeds where the tooth passing frequency is equal to an integer fraction of the system natural frequency which corresponds to the most flexible mode (these are the traditionally-selected 'best' speeds which are located near the lobe peaks in stability lobe diagrams). *Figure 4* shows a stability lobe diagram, which describes the allowable axial depth of cut as a function of the spindle speed. Any (Ω, *b*) combination which lies above the boundary, represented by a heavy dashed line, gives chatter, or unstable cutting conditions. The diagram also gives the values of the objective functions: constant material removal rate is seen along the dotted f_{MRR} lines and the surface location error magnitude is given by the thin $\left|f_{SLE}\right|$ lines. The optimum points obtained using SQP are superimposed on the plot (circles).

Because f_{SLE} can undergo large changes in value for small perturbations in Ω at the optimum points, the formulation provided in Eqs. (6)-(8) leads to optima which are highly sensitive to spindle speed variation. The Pareto front shown in *Figure 5* gives the value of the objective functions of the optimum points found using this SQP approach. The 'optimal' set is shown to converge on dominated optima (local), which are not part of the Pareto front. The only non-dominated optima are located at {250 and 350} mm^3/s. To show the sensitivity of these optimum points, a typical optimum point is superimposed on a graph of $\left|f_{SLE}\right|$ vs. Ω in *Figure 6*. It is seen that the optimum point is located in a high f_{SLE} slope region.

Therefore, the optimization problem was redefined in order to avoid convergence to these points. Two approaches were applied: 1) an additional constraint was added to the $\left|f_{SLE}\right|$ slope; and 2) the f_{SLE} objective was redefined as the average of three perturbed spindle speeds. The latter proved to be more robust than the former. Therefore, Eq.(7) was redefined as:

$$\frac{\left|f_{SLE}\left(x_1, x_2 + \delta\right)\right| + \left|f_{SLE}\left(x_1, x_2\right)\right| + \left|f_{SLE}\left(x_1, x_2 - \delta\right)\right|}{3} \le \varepsilon_i \quad \text{for } i = 1, ..., k \tag{9}$$

where δ is the spindle speed perturbation selected by the designer (a typical value for our analyses was 50 rpm).

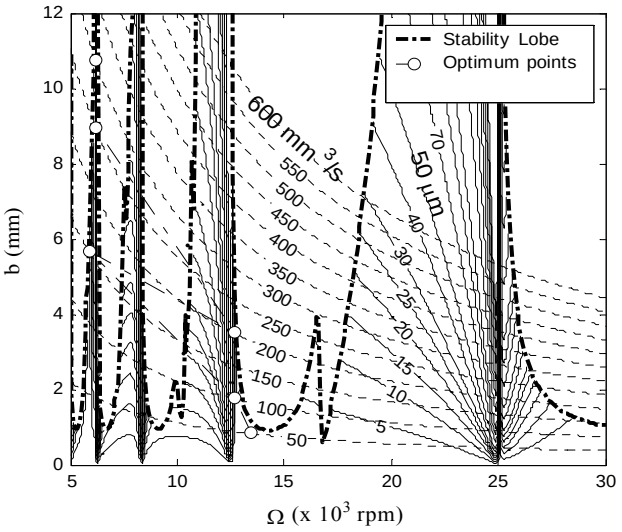

Figure 4. Stability, $|f_{SLE}|$ and f_{MRR} contours with optimum points found using optimization statement in Eqs. 6-8. The figure shows that optimum points occur in regions sensitive to spindle speed variation.

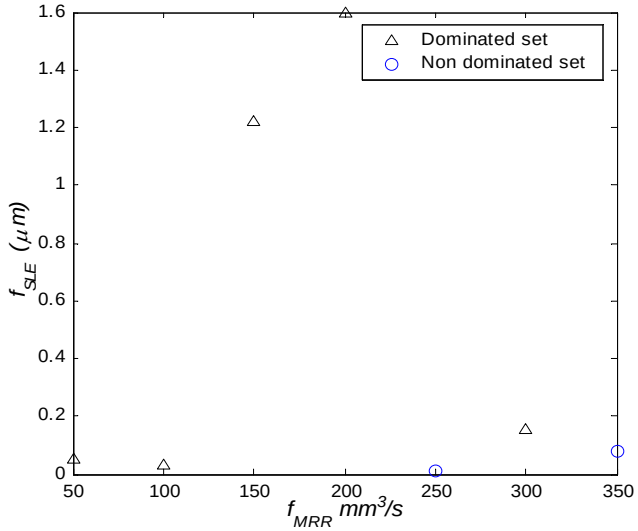

Figure 5. Pareto front for original problem defined by Eqs. 6-8, the non-dominated points are on Pareto front.

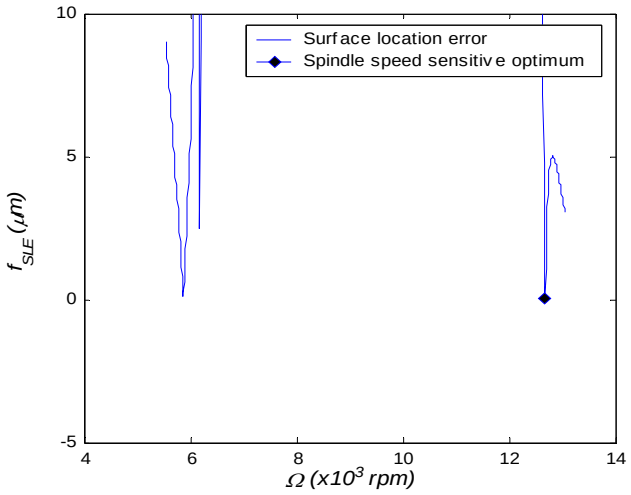

Figure 6. A typical optimum point found using Eqs. 6-8; optimum point sensitivity with respect to spindle speed is apparent.

The optimization problem can be expressed in a reverse manner as well. That is, the objective function can be defined as the average of $|f_{SLE}|$ as shown in Eq. (9) and the optimization problem can be solved for a different set of constraints on f_{MRR}. Solution of this optimization problem statement using the SQP method converged to optimum points that are relatively insensitive to spindle speed variation, as shown in *Figure 7*.

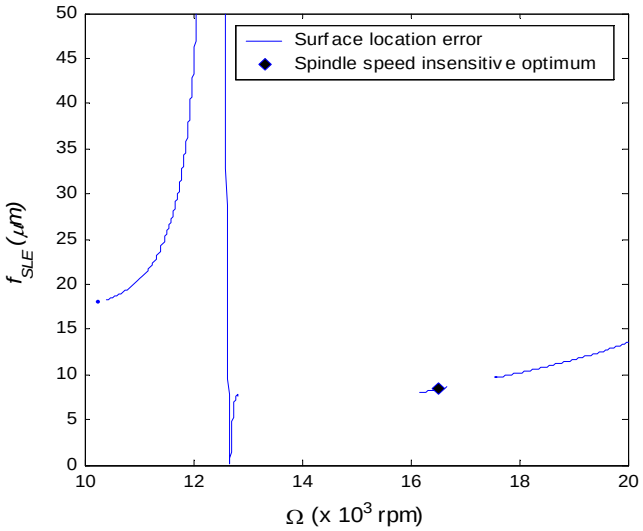

Figure 7. A typical optimum point (200 mm3/s) found using the modified optimization problem is shown; it is insensitive to spindle speed.

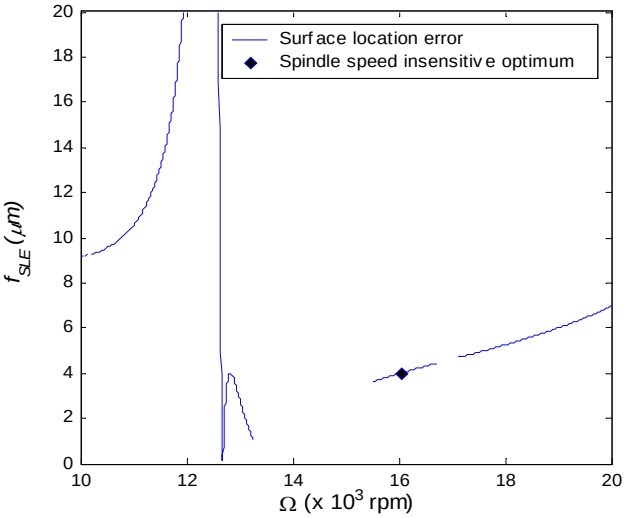

Figure 8. Typical optimum point found using PSO (4µm constraint); relative insensitivity to spindle speed is noted.

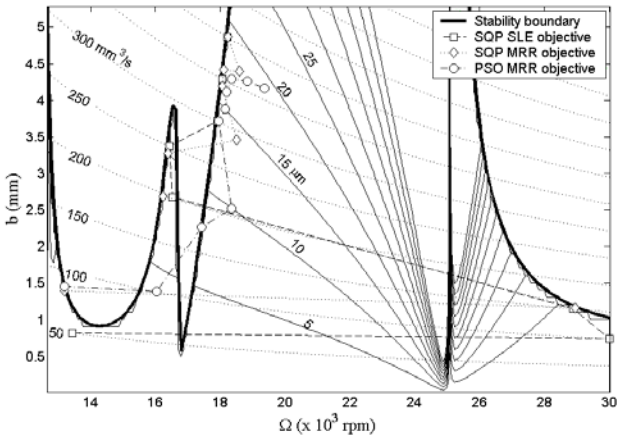

Figure 9. Stability, fSLE, and fMRR contours with optimum Pareto front points found using PSO and SQP with and average perturbed respectively. The figure shows that optimum points are not in regions sensitive to spindle speed.

In comparison, when using the PSO method the objective function - f_{MRR} was minimized for a set of different constraints on $|f_{SLE}|$ as shown in Eq. (7), rather than its perturbed average as defined in Eq. (9). In the PSO method, the optimum points didn't converge on highly f_{SLE} sensitive points; an example point is shown in *Figure 8*. A comparison of the three optimization schemes is shown in *Figure 9* and *Figure 10*. *Figure 9* shows the optima for each approach superimposed on the corresponding stability lobe diagram. In *Figure 10*, the Pareto fronts for the three methods are shown. The optimum points found using the two SQP formulations closely agree.

Although the PSO points show the same trend, some improvement in the fitness is still possible relative to the SQP results. Because the PSO search avoided optimum points that are spindle speed sensitive, computational time can be reduced using this global search method. However, narrow optimum points may go undetected when using this approach.

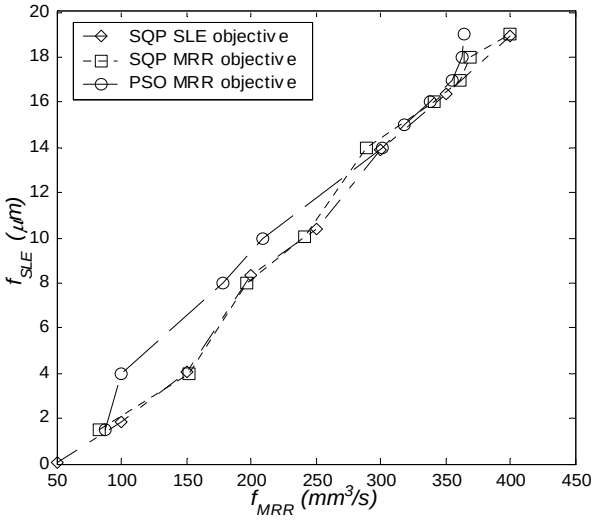

Figure 10. Pareto front showing optimum points found using three optimization algorithms/formulations; the same trends are apparent. However, the SQP methods required additional computational time.

As noted, when comparing the Pareto fronts in *Figure 10*, it is seen that the PSO approach did not converge to the same fitness as SQP method. A check of the optimum points which correspond to a value of $|f_{SLE}|$ = 4 µm, for example, shows that PSO converged to 100 mm^3/s, while SQP converged to 150 mm^3/s. To better understand this result, the design space was divided between the two design vectors, *b* and Ω, for SQP and PSO using a factor, *a*, that was normalized between 0 and 1. The PSO and SQP optimums were normalized to *a* = 0 and 1 respectively. Next, the stability constraint (eigenvalue), material removal rate and $|f_{SLE}|$ was plotted against that ratio. In *Figure 11* it is seen that discontinuities exist in the $|f_{SLE}|$ constraint and first derivative of the eigenvalue constraint within this region. Although PSO is not affected much by a discontinuity in the derivative constraint, it can be affected by a discontinuity of the $|f_{SLE}|$ constraint, where the discontinuity tends to narrow the search region of the swarm.

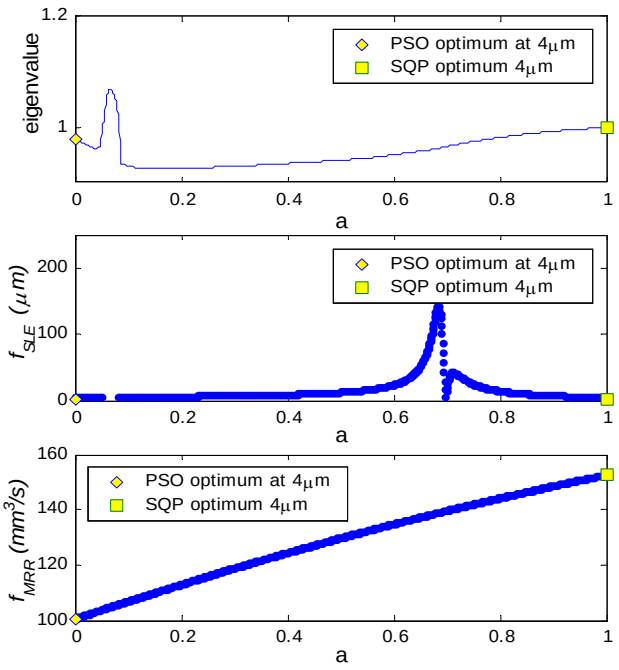

Figure 11. Variations in the eigenvalues, surface location error, and removal rate for PSO and SQP optima, where f_{MRR} is the objective for both. The discontinuities in the surface location error and first derivative of the stability constraint (eigenvalue) cause PSO to not converge on the SQP optimum.

Although SQP in both variations of the objective function and constraint converged to approximately the same optima, the one with the average perturbed $|f_{SLE}|$ constraint required a large number of initial guesses in order to converge to the same optimum as the SQP with the f_{MRR} constraint approach. This can be attributed to the low damping in the dynamic system used in this study which makes the $|f_{SLE}|$ contours (constraint) quite steep.

Table 1: Modal parameters for 19.05 mm diameter tool used in optimization simulations and cutting tests.

M (kg)		**C** (N-s/m)		**K** (N/m)	
0.061	0	3.86	0	1.67×10^6	0
0	0.056	0	3.94	0	1.52×10^6

4 EXPRIMENTAL VERIFICATION

To validate the TFEA stability boundary and accuracy predictions, milling tests were performed using a compliant 19.05 mm diameter tool as shown in *Figure 12* [41]. The modal parameters for the tool are listed in Table 1.

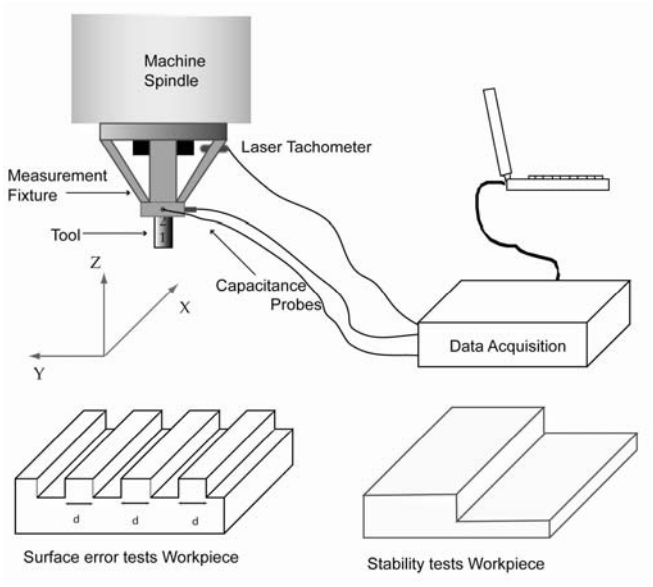

Figure 12. Schematic of test setup and machined blocks used for stability and surface location error tests.

4.1 Stability boundary tests

The stability boundary was verified by performing 5% radial immersion down milling tests on an aluminum (7050-T7456) block. Cuts were completed at different axial depths and spindle speeds and the tool displacement was recorded during each test. A cut was declared stable if the 1/tooth-sampled displacement approached a constant value [45]. The cutting test results are overlaid on the TFEA stability boundary in *Figure 13*. Good agreement is seen.

4.2 Surface accuracy tests

The TFEA accuracy predictions were verified by machining the 250 mm long islands (see *Figure 12*) on the aluminum block to a final width, *d*, of 19.05 mm using a constant axial depth (2.03 mm) and chip load (0.18 mm/tooth) with different spindle speeds for each island. A coordinate measuring machine (CMM) was used to measure $\left|f_{SLE}\right|$ at six different locations along each island (near the middle portion of each island).

The average $\left|f_{SLE}\right|$ values measured by the CMM are shown together with the predicted surface location error in *Figure 14*; good qualitative agreement is evident.

To compare the optimization results with the CMM measurements, the SQP optimization was modified to consider only spindle speed as the design variable (the axial depth was set equal to the depth used for the surface error tests). The optimum points are included in *Figure 14*, where they show good correspondence with CMM measurement trends.

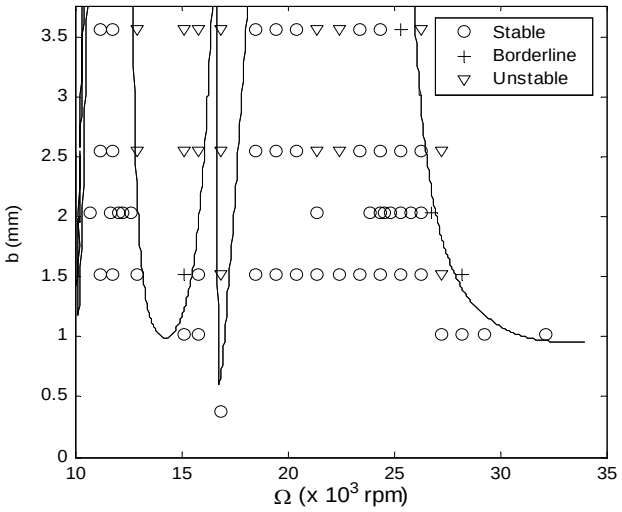

Figure 13. Down-milling experimental results vs. TFEA stability boundary for 19.05 mm tool.

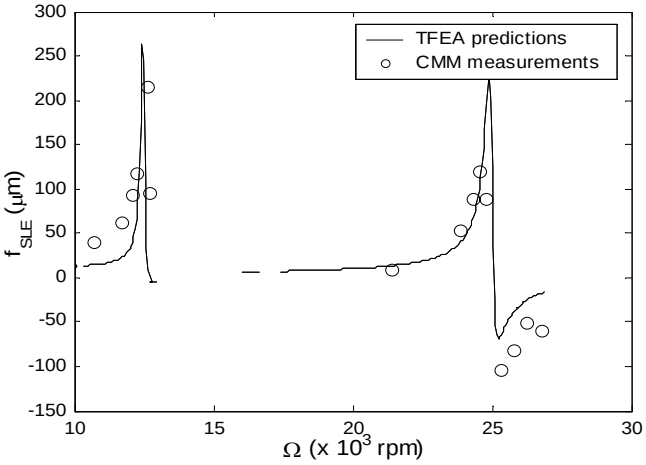

Figure 14. TFEA surface location error prediction vs. CMM measured error and optimum points.

5 CONCLUSIONS

This paper describes initial efforts toward the multi-objective optimization of high-speed milling. Material removal rate and surface location error were considered to arrive at a set of optimum operating conditions, referred to as the Pareto front. Consideration was given to the practical issue of convergence to optima near regions of high sensitivity of surface location error to spindle speed variations. Experimental results were provided and good agreement with prediction was seen.

ACKNOWLEDGMENTS

The authors acknowledge financial support from the National Science Foundation (DMI-0238019 and CMS-

0348288) and Office of Naval Research (2003 Young Investigator Program).

REFERENCES

1. Ermer, D.S., *Optimization of Constrained Machining Economics Problem by Geometric Programming.* ASME Journal of Engineering for Industry, 1971. **93**: p. 1067-1072.
2. Hati, S.K. and S.S. Rao, *Determination of Optimum Machining Conditions -Deterministic and Probabilistic Approaches.* ASME Journal of Engineering for Industry, 1975. **98**: p. 354-359.
3. Hitomi, K., *Analysis of Optimal Machining Speeds for Automatic Manufacturing.* Int. J. Production. Research, 1989. **27**: p. 1685-1691.
4. Shalaby, M.A. and M.S. Riad. *A Linear Optimization Model for Single Pass Turning Operations*. in *Proc. 27th Int. MATADOR Conf*. 1988.
5. Boothroyd, G. and P. Rusek, *Maximum Rate of Profit Criteria in Machining.* ASME Journal of Engineering for Industry, 1976. **98**: p. 217-220.
6. Wu, S.M. and D. Ermer, *Maximum Profit as the Criterion in the Determination of the Optimum Cutting Conditions.* ASME Journal of Engineering for Industry, 1966. **88**: p. 435-442.
7. Agapiou, J.S., *The Optimization of Machining Operations Based on a Combined Criterion - Part I: The Use of Combined Objectives in Single-Pass Operations.* ASME Journal of Engineering for Industry, 1992. **114**: p. 500-507.
8. Abuelnaga, A.M. and M.A. Eldardiry, *Optimization Methods for Metal-Cutting.* International Journal of Machine Tools & Manufacture, 1984. **24**(1): p. 11-18.
9. Ermer, D.S. and D.C. Patel. *Maximization of the Production Rate with Constraints by Linear Programming and Sensitivity Analysis*. in *Proc. NAMRC*. 1974.
10. Milner, D.A., *Use of Linear-Programming for Machinability Data Optimization.* Mechanical Engineering, 1977. **99**(7): p. 96-96.
11. Challa, K. and P.B. Berra, *Automated Planning and Optimization of Machining Processes: A Systems Approach.* Comput. Indus. Engr., 1976. **1**: p. 35-45.
12. Giardini, C., A. Bugini and R. Pagagnella, *The Optimal Cutting Conditions as a Function of Probability Distribution Function of Tool Life and Experimental Test Numbers.* International Journal of Machine Tools and Manufacture, 1988. **28**: p. 453-459.
13. Iwata, K., Y. Murostu, I. T. and S. Fujii, *A probabilistic Approach to the Determination of the Optimum Cutting.* ASME Journal of Engineering for Industry, 1972. **94**: p. 1099-1107.
14. Sheikh, A.K., L.A. Kendall and S.M. Pandit, *Probabilistic Optimization of Multitool Machining Operations.* ASME Journal of Engineering for Industry, 1980. **102**: p. 239-246.
15. Beightler, C.S. and D.T. Philips. *Optimization in Tool Engineering Using Geometric Programming*. in *AIIE Trans*. 1970.
16. Eskicioglu, H., M.S. Nisli and S.E. Kilic. *An Application of Geometric Programming to Single-Pass Turning Operations*. in *Proceedings of International MTDR Conference*. 1985. Birmingham.
17. Gopalakrishnak, B. and F. Al-Khayyal, *Machine Parameter Selection for Turning with Constraints: An Analytical Approach Based on Geometric Programming.* International Journal of Production Research, 1991. **29**: p. 1897-1908.
18. Petropoulos, P.G., *Optimal Selection of Machining Rate Variables by Geometric Programming.* International Journal of Production Research, 1975. **13**: p. 390-395.
19. Walvekar, A.G. and B.K. Lambert, *An Application of Geometric Programming to Machining Variable Selection.* International Journal of Production Research, 1970. **8**: p. 241-245.
20. Hough, C.L. and R.E. Goforth. *Optimization of the Second-Order Logarithmic Machining Economics Problem by Extended Geometric Programming*. in *AIIE Transactions*. 1981.
21. Fischer, G.W., Y. Wei and S. Dontamsetti, *Process-Controlled Machining of Gray Cast Iron.* Journal of Mechanical Working Tech. 20, 1989. **20**: p. 47-57.
22. Philipson, R.H. and A. Ravindran, *Application of Goal Programming to Machinability Data Optimization.* ASME Journal of Mechine Design, 1978. **100**: p. 286-291.
23. Sundaram, R.M., *An Application of Goal Programming Technique in Metal Cutting.* International Journal of Production Research, 1978. **16**: p. 375-382.
24. Subbarao, P.C. and C.H. Jacobs. *Application of Nonlinear Goal Programming to Machining Variable Optimization*. in *Proc. NAMRC*. 1978.
25. Dubois, D. *A Fuzzy-Set-Based Method for the Optimization of Machining Operations*. in *Proceedings of International Conference on Cybernetics and IEEE Systems*. 1981: Man and Cybernetics Society.
26. Fang, X.D. and I.S. Jawahir, *Predicting Total Machining Performance in Finish Turning Using Integrated Fuzzy-Set Models of the Machinability Parameters.* International Journal of Production Research., 1994. **32**: p. 833-849.
27. Tandon, V., H. El-Mounayri and H. Kishawy, *NC end milling optimization using evolutionary computation.* International Journal of Machine Tools and Manufacture, 2002. **42**(5): p. 595-605.

28. Jha, N.K., *A Discrete Data Base Multiple Objective Optimization of Milling Operation Through Geometric Programming.* ASME Journal of Engineering For Industry, 1990. **112**: p. 368.
29. Koulams, C.P., *Simultaneous Determination of Optimal Machining Conditions and Tool Replacement Policies In Constrained Machining Economics Problem By Geometric Programming.* International Journal of Production Research, 1991. **29**(12): p. 2407-2421.
30. Armarego, E.J.A., A.J.R. Smith and J. Wang, *Constrained Optimization Strategies And CAM Software For Single-Pass Peripheral Milling.* International Journal of Production Research, 1993. **31**(9): p. 2139-2160.
31. Armarego, E.J.A., A.J.R. Smith and J. Wang, *Computer-Aided Constrained Optimization Analyses And Strategies For Multi-pass Helical Tooth Milling Operations.* CIRP Annals, 1994. **43**(1): p. 437.
32. Akturk, M.S. and S. Avci, *Theory And Methodology Tool Allocation And Machining Conditions Optimization For CNC Machines.* European Journal of Operational Research, 1996. **94**: p. 335.
33. Sonmez, A.I., A. Baykasoglu, D. Turkay and I.H. Filiz, *Dynamic Optimization Of Multi-Pass Milling Operations Via Geometric Programming.* International Journal of Machine Tools & Manufacture, 1999. **39**(2): p. 297-320.
34. Wang, J. and E.J.A. Armarego, *Computer-Aided Optimization Of Multiple Constraint Single Pass Face Milling Operations.* Machining Science and Technology, 2001. **5**(1): p. 77-99.
35. Lin, T.-R., *Optimization Technique for Face Milling Stainless Steel With Multiple Performance Characteristics.* International Journal of Advanced Manufacturing Technology, 2002. **19**: p. 330-335.
36. Kim, K.-K., M.-C. Kang, J.-S. Kim, et al., *A Study On The Precision Machinability Of Ball End Milling By Cutting Speed Optimization.* Journal of Materials Processing Technology, 2002. **130-131**: p. 357-362.
37. Juan, H., S.F. Yu and B.Y. Lee, *The optimal cutting-parameter selection of production cost in HSM for SKD61 tool steels.* International Journal of Machine Tools & Manufacture, 2003. **43**(7): p. 679-686.
38. Lu, J., O.B. Ozdoganlar, S.G. Kapoor and R.E. DeVor. *A Process Model Based Methodology For Comprehensive Process Planning of Contour Turning Operations*. in *Transactions of NAMRI/SME*. 2003.
39. Schwier, A.S., *Manual of Political Economy, Translation of the French Edition (1927)*. 1971, London-Basingslohe: McMillan Press Ltd.
40. Kalyanmoy, D., *Multi-Objective Optimization Using Evolutionary Algorithms*. 2001, West Sussex, England: John Wiley.
41. Mann, B.P., *Dynamics of Milling Process*. 2003, Washington University: Saint Louis, Mo.
42. Mann, B.P., P.V. Bayly, M.A. Davies and J.E. Halley, *Limit Cycles, Bifurcations, and Accuracy of the Milling Process.* Journal of Sound and Vibration, 2004: p. in press.
43. Mann, B.P., T. Insperger, P.V. Bayly and G. Stepan, *Stability of up-milling and down-milling, Part 2: Experimental verification.* International Journal of Machine Tools and Manufacture, 2003. **43**: p. 35-40.
44. Insperger, T., B.P. Mann, G. Stepan and P.V. Bayly, *Stability of up-milling and down-milling, Part1: Alternative analytical methods.* International Journal of Machine Tools and Manufacture, 2003. **43**: p. 25-34.
45. Halley, J.E., *Stability of Low Radial Immersion Milling*. 1999, Washington University: St. Louis, Mo.
46. Eschenauer, H.A., J. Koski and A. Osyczka, *Multicriteria Design Optimization: Procedures and Applications*. 1986, NY: Springer-Verlag.
47. Hu, X. and R. Eberhart. *Solving constrained nonlinear optimization problems with particle swarm optimization*. in *6th World Multiconference on Systemics, Cybernetics and Informatics*. 2002. Orlando, USA.
48. Wu, J. and S. Azarm, *Metrics for Quality Assessment of a Multiobjective Design Optimization Solution Set.* Journal of Mechanical Design, 2001. **123**: p. 18-25.